Phytochemistry 179 (2020) 112469

Contents lists available at ScienceDirect

Phytochemistry

journal homepage: www.elsevier.com/locate/phytochem

Cytotoxic sesquiterpene lactones from *Campuloclinium macrocephalum* (=*Eupatorium macrocephalum*)

Márcia R. Pereira Cabral[a], Mariana Cecchetto[b], João M. Batista Jr.[c], Andrea N.L. Batista[d], Mary Ann Foglio[b], Ana Lúcia Tasca Gois Ruiz[b], Marta R. Barrotto do Carmo[e], Willian Ferreira da Costa[a], Débora C. Baldoqui[a], Maria H. Sarragiotto[a,*]

[a] *Departamento de Química, Universidade Estadual de Maringá, Av. Colombo 5790, 87020-900, Maringá, PR, Brazil*
[b] *Faculdade de Ciências Farmacêuticas, Universidade Estadual de Campinas, R. Candido Portinari 200, Cidade Universitária, 13083871, Campinas, SP, Brazil*
[c] *Instituto de Ciência e Tecnologia, Universidade Federal de São Paulo, R. Talim 330, 12231-280, São José dos Campos, SP, Brazil*
[d] *Instituto de Química, Universidade Federal Fluminense, Outeiro de São João Batista s/n, 24020-141, Niterói, RJ, Brazil*
[e] *Departamento de Biologia Geral, Universidade Estadual de Ponta Grossa, Av. Carlos Cavalcanti, 4748, 84030-910, Ponta Grossa, PR, Brazil*

A R T I C L E I N F O

Keywords:
Campuloclinium macrocephalum
Asteraceae
Sesquiterpene lactones
Germacranolide
Cytotoxicity

A B S T R A C T

Three undescribed germacranolide sesquiterpene lactones, named macrocephalides **A-C**, along with known steroids, triterpenes and flavonoids were isolated from the aerial parts of *Campuloclinium macrocephalum.* The structures of the undescribed compounds were elucidated with basis on their 1D and 2D-NMR, and HR-ESI-MS data. Their absolute configurations were assigned by comparison of experimental and calculated electronic circular dichroism (ECD) spectra. Additionally, macrocephalides **A-C** were evaluated for their *in vitro* cytotoxic activities against nine human cancer cell lines. Macrocephalides A and B exhibited moderate to potent cytotoxic activity, inhibiting 50% of cell growth (GI_{50}) at concentrations ranging from 0.576 to 6.37 μM.

1. Introduction

Campuloclinium macrocephalum (Less.) DC (synonymy *Eupatorium macrocephalum* Less.), belongs to the family Asteraceae, tribe Eupatorieae, and is a perennial herb widely distributed in the New World, from Mexico to Argentina (Cabrera, 1974). This species originates from South America (Williams, 1976; Cabrera, 1978; Breedlove, 1986), being distributed in Brazil, Bolivia, Paraguay, Uruguay and north of Argentina (Freire, 2008). The taxon was introduced to South Africa, in the 1970s, where is known as “pompom weed”, and has being described as an invader of grasslands, wetlands and roadsides in several provinces (Goodall et al., 2010). On the other hand, this species is reported to be used in Paraguayan folk medicine as anti-inflammatory, sedative and in treatment of cardiac disease (Gonzalez, 1992).

The literature reports few studies concerning biological activity and chemical composition of *C. macrocephalum.* In a study conducted by Goodall et al. (2010) the role of its allelopathic effect and competition in invasiveness was investigated using *Eragrostis curvula* (weeping lovegrass, an indigenous grass), *E. tef* and *Lactuca sativa* (lettuce) as test species (Goodall et al., 2010). Root and shoot extracts of *C. macrocephalum* did not inhibit seed germination of any tested species. The antifungal activities of leaf and flower extracts of *C. macrocephalum* were evaluated against phytopathogenic fungi (Mdee et al., 2009). The leaf extract showed higher activity than that of the extract of flowers, presenting potent activity against *Colletotrichum gloeosporioides* (MIC of 0.05 mg mL^{-1}).

The chemical studies on *C. macrocephalum*, under the synonymy *Eupatorium macrocephalum* Less., reported the isolation and identification of triterpenes, steroids, cinnamic acid derivatives, and flavonoids (Gonzalez et al., 1972, 1973; Vega et al., 2008). However, to the best of our knowledge, no studies to date have reported the isolation of sesquiterpene lactones from this species. Sesquiterpene lactones (SLs) constitute an important group of specialized products widely distributed in various genus of Asteraceae, including *Eupatorium* (Huo et al., 2004; Shen et al., 2005; Zhang et al., 2008; Hensel et al., 2011; Saito et al., 2014; Liu et al., 2015; Wang et al., 2018; Yu et al., 2018), the genus to which belonged the species *C. macrocephalum*. *Eupatorium* species extracts and their isolated sesquiterpene lactones have been reported to exhibit cytotoxic activities against different cancer cell lines (Huo et al., 2004; Shen et al., 2005; Hensel et al., 2011; Saito et al., 2014; Yu et al.,

* Corresponding author.
E-mail address: mhsarragiotto@uem.br (M.H. Sarragiotto).

https://doi.org/10.1016/j.phytochem.2020.112469
Received 28 March 2020; Received in revised form 27 June 2020; Accepted 23 July 2020
Available online 14 August 2020

2018).

In the present study, three undescribed germacranolide sesquiterpene lactones, named macrocephalides A, B and C (**1**–**3**), along with known steroids and triterpenes (**4**–**10**), and the flavonoids taxifolin (**11**) and quercetin-3-*O*-*α*-L-rhamnopyranoside-7-*O*-*β*-D-glucopyranoside (**12**) were isolated from the aerial parts of *C. macrocephalum*. Additionally, the *in vitro* cytotoxic activities of the germacranolides **1**–**3** against nine human cancer cell lines were evaluated. Herein, the isolation, structure elucidation including absolute stereochemistry assignment, and the cytotoxic activities of the undescribed compounds **1**–**3** are described.

2. Results and discussion

2.1. Isolation and structure elucidation

A crude methanol extract of the aerial parts of *C. macrocephalum* was subjected to partition into *n*-hexane, dichloromethane and ethyl acetate. Purification of the dichloromethane fraction on silica gel *flash* chromatography column afforded compounds **1**–**3** (Fig. 1). The *n*-hexane fraction yielded known steroids and triterpenes, after purification by CC on silica gel. The compounds were identified as lupeol acetate (**4**), α-amyrin acetate (**5**), β-amyrin acetate (**6**), lupeol (**7**), α-amyrin (**8**), β-amyrin (**9**) and pseudotaraxasterol (**10**) by comparison of their spectroscopic data with those reported (Mahato and Kundu, 1994; Vega et al., 2008). Compounds **4**–**9** were earlier reported from *C. macrocephalum* (Vega et al., 2008). Purification of the ethyl acetate fraction in Sephadex LH-20 afforded the flavonoids taxifolin (**11**) and quercetin-3-*O*-*α*-L-rhamnopyranoside-7-*O*-*β*-D-glucopyranoside (**12**) (Agrawal, 1989).

Compound **1**, named macrocephalide A, was isolated as an oil with $[\alpha]_D^{24}$ −117 (*c* 0.7, $CHCl_3$). Its molecular formula was determined as $C_{22}H_{26}O_9$ based on the protonated molecular ion at *m/z* 435.1651 $[M+H]^+$ (calcd for $C_{22}H_{27}O_9$ *m/z* 435.1650) in the HR-ESI-MS spectra. The ^{1}H-NMR spectrum of **1** displayed characteristic resonances of an α-methylene-γ-lactone group at δ_H 6.26 (d, J = 1.5 Hz, H-13a) and δ_H 5.71 (d, J = 1.5 Hz, H-13b), three oxymethyne hydrogens at δ_H 6.02 (d, J = 9.5 Hz, H-6), δ_H 5.45 (dd, J = 4.0 and 3.0 Hz, H-8) and δ_H 4.34 (t, J = 3.0 Hz, H-9), and two methyl groups at δ_H 1.65 (14-CH_3) and δ_H 1.92 (15-CH_3). The ^{13}C NMR data confirmed the presence of a α-methylene-γ-lactone moiety (Table 1) due the signals at δ_C 136.0 (C-11), 169.8 (C-12) and δ_C 124.2 (C-13). Among others, the ^{13}C NMR spectrum showed signals for a carbonyl group at δ_C 206.3 (C-1), oxygenated carbons at δ_C 75.4 (C-6), δ_C 75.4 (C-8), δ_C 75.5 (C-9) and δ_C 79.9 (C-10) and for methyl groups at δ_C 26.3 (CH_3-14) and δ_C 21.8 (CH_3-15). Comparison of these data with those of literature for calealactones A and C indicated that compound **1** is a germacranolide, containing an α-methylene-γ-lactone group and oxygenated substituents at C-8 and C-9 (Yamada et al., 2004; Wu et al., 2011).

Table 1
^{1}H (500 MHz) and ^{13}C (125 MHz) NMR data of compounds **1**–**3** in $CDCl_3$ (*δ* in ppm, *J* in Hz).

position	1		2		3	
	δ_H	δ_C	δ_H	δ_C	δ_H	δ_C
1	–	206.3	–	206.4	–	150.7
2	6.73, d (12.0)	131.1	6.70, d (11.5)	131.1	5.72, d (5.5)	105.4
3	6.29, d (12.0)	137.7	6.29, d (11.5)	137.6	5.87, m	117.5
4	–	136.2	–	136.3	–	133.6
5	5.06, dquint (9.5, 1.0)	125.7	5.07, dquint (9.0, 1.5)	125.6	4.15, d (9.0)	76.6
6	6.02, brd (9.5)	75.4	6.03, brd (9.0)	75.5	4.93, t (9.0)	79.5
7	2.86, m	45.2	2.88, m	44.9	3.38, m	49.2
8	5.45, dd (4.0, 3.0)	75.4	5.39, dd (4.5, 3.0)	75.6	5.87, m	75.0
9	4.34, t (3.0)	75.5	4.31, d (3.0)	76.5	4.4, brs	80.6
10	–	79.9	–	79.9	–	74.1
11	–	136.0	–	136.2	–	134.3
12	–	169.8	–	170.1	–	168.4
13	6.26, d (1.5) 5.71, d (1.5)	124.2	6.28, d (1.5) 5.73, d (1.5)	124.1	6.39, d (3.0) 5.75, d (3.0)	122.9
14	1.65 (s)	26.3	1.61 (s)	26.3	1.30 (s)	18.5
15	1.92 (brs)	21.8	1.92 (s)	21.8	2.02 (d, 1.5)	19.8
1′	–	163.8	–	163.9	–	167.5
2′	–	127.4	–	131.0	–	130.5
3′	6.46, q (7.5)	147.7	6.30, q (7.5)	143.7	6.47, q (7.5)	143.6
4′	2.02, d (7.5)	15.8	2.04, dd (7.0, 1.5)	15.5	2.00, d (7.5)	15.9
5′	4.56, d (12.0) 4.91, d (12.0)	65.4	4.07, d (11.5) 4.51, dt (11.5, 1.5)	66.0	4.13, d (11.5) 4.17, d (11.5)	64.1
1″	–	171.6	–			
2″	2.08 (s)	21.1				

Differently from calealactones, compound **1** showed signals at δ_H 6.29 (d, J = 12.0 Hz, 1H, H-3), 6.73 (d, J = 12.0 Hz, 1H, H-2), correlated in the COSY spectra, and at 5.06 (dquint, J = 9.5 and 1.0 Hz, 1H, H-5), which were consistent with the presence of double bonds between C-2/C-3 and C-4/C-5 (Table 1). The connectivity for germacranolide skeleton was deduced by the COSY correlations between the hydrogens at δ_H 6.73

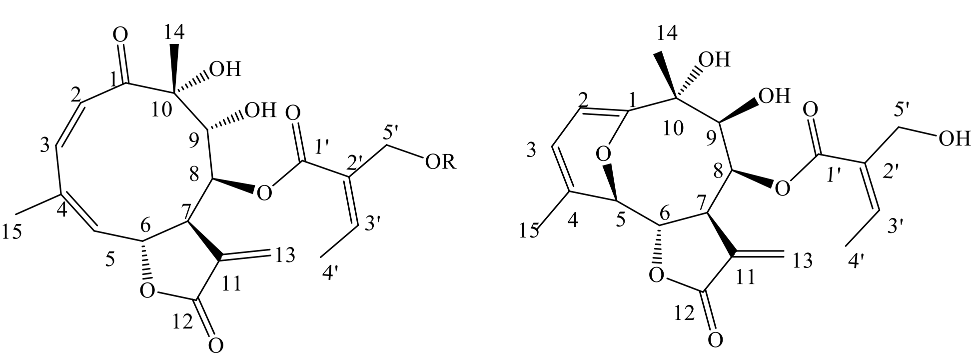

1 R = Ac
2 R = H

3

Fig. 1. Structures of compounds **1**–**3**.

(H-2) with δ_H 6.29 (H-3), δ_H 5.06 (H-5) with δ_H 6.02 (H-6), δ_H 2.86 (H-7) with δ_H 5.45 (H-8), and at δ_H 5.45 (H-8) with δ_H 4.34 (H-9) (Figures S-9 and S-10, Supporting Information). The 2.4-dienone system was evidenced in the ^{13}C NMR spectra by the signals at δ_C 206.3 (C=O), 131.1 (C-2), 137.7 (C-3), 136.2 (C-4) and 125.7 (C-5). The correlations observed in HMBC spectra of H-3 (δ_H 6.29) with the carbonyl group (δ_C 206.3, C-1), and of H-5 (δ_H 5.06) with C-3 (δ_C 137.7), corroborated the assignment of carbons and hydrogens of this system (Figures S-7 and S-8, Supporting Information).

The linkage of the methyl groups to C-4 and C-10 of the germacranolide skeleton was supported by the HMBC correlations of hydrogens at δ_H 1.92 (15-CH_3) and δ_H 1.65 (14-CH_3) with C-5 (δ_C 125.7) and C-1 (δ_C 206.3), respectively (Fig. 2).

The oxymethylene hydrogens at δ_H 4.91 (d, $J = 12.0$ Hz, H-5′) and δ_H 4.56 (d, $J = 12.0$ Hz, H-5′), methyl groups at δ_H 2.02 (d, $J = 7.5$ Hz, H-4′) and 2.08 (s, H-2″), and an β-hydrogen of a α,β-unsaturated ester group at δ_H 6.46 (q, $J = 7.5$ Hz, H-3′) could be attributed to the substituent attached to C-8 of the germacranolide skeleton. The carbons at δ_C 163.8 (C-1′), 127.4 (C-2′), 147.7 (C-3′), δ_C 15.8 (C-4′) and 65.4 (C-5′), together with the acetoxy group at δ_C 171.6 (C=O) and 2.02 (CH_3) evidenced the presence of a 2-acetoxymethyl-2-butenoyl group in compound **1**. HMBC correlations of H-5’ (δ_H 4.91 and 4.56) with the carbonyl groups at δ_C 163.8 (C-1′) and 171.6 (C-1”) confirmed the attachment of the acetoxy group to C-5’. The positioning of this 2-acetoxymethyl-2-butenoyl group at C-8 was deduced from the HMBC correlations of H-6 (δ_H 6.02) and H-8 (δ_H 5.45) with the carbons at δ_H 75.4 (C-8) and at δ_C 163.8 (C-1’), respectively.

The NOESY spectra of compound **1** showed correlation of H-9 (δ_H 4.34) with H-14 (δ_H 1.65), indicating that H-9 and methyl group at C-10 are in the same face of the molecule. The α-orientation of the hydroxyl groups at C-9 and C-10, and consequent β-orientation of H-9 and methyl group at C-10, were based on NOESY experiment and corroborated by literature for compounds with similar germacranolide skeleton (Yamada et al., 2004; Wu et al., 2011).

The geometries of the C-4/C-5 and C-2’/C-3′ double bonds were suggested as *Z* due to the NOESY correlations of H-5 (δ_H 5.06) with the methyl group CH_3-15 (δ_H 1.92), and of H-3′(δ_H 6.46) with the methylene hydrogens H-5’ (δ_H 4.91; δ_H 4.56), respectively (Fig. 3). After securing the relative configuration of compound **1**, comparisons of experimental ECD data with time-dependent density functional theory (TDDFT) simulated spectra were performed to determine its absolute configuration. The good agreement between observed and calculated (Fig. 4) data allowed the assignment of (−)-**1** as 6*R*,7*S*,8*S*,9*R*,10*R*. The small positive Cotton effect at around 260 nm was not reproduced by the calculations due to oppositely signed contributions from different conformers (ESI).

Compound **2**, macrocephalide B, was isolated as an oil with $[\alpha]_D^{24}$ −150 (*c* 0.4, $CHCl_3$). The HR-ESI-MS spectra showed a protonated molecular ion at *m/z* 393.1543 $[M+H]^+$, supporting its molecular formula to be $C_{20}H_{24}O_8$ (calcd for $C_{20}H_{25}O8$ *m/z* 393.1544). The ^{1}H and ^{13}C NMR data of **2** showed a close structural resemblance to that of **1**, except for the absence of signals for the acetoxy group [δ_H 2.08 (H-2″), δ_C 21.1 (C-2″) and δ_C 171.6 (C-1″)] and its replacement by a hydroxyl group, as evidenced by the shielding of H-5’ signals, which appear at δ_H 4.07 and 4.51 for **2**, and at δ_H 4.56 and 4.91 for compound **1**. Based on these data, the substituent at C-8 of compound **2** was determined to be the 2-hydroxymethyl-2-butenoyl, which was confirmed by the signals at δ_C 163.9 (C = 0), δ_C 131.0 (C-2′), δ_C 143.7 (C-3′), δ_C 15.5 (C-4′) and δ_C 66.0 (C-5′) in the ^{13}C NMR spectra. These findings were consistent with the difference of 42 units in the protonated ion molecular of **2** (*m/z* 393.1544 $[M+H]^+$) compared to that of compound **1** (*m/z* 435.1651 $[M+H]^+$) (Figure S-12, Supporting Information). The position of the 2-hydroxymethyl-2-butenoyl group at C-8 was confirmed by HMBC correlations (Figures S-17 and S-18, Supporting Information) of H-8 (δ_H 5.39) with C-1’ (δ_C 163.9) (Fig. 2).

The NOESY correlations of compound **2** (Figure S-21, Supporting Information) were similar as those observed for compound **1**, which supported the same relative configuration for both compounds. The very good correlation between experimental and calculated ECD data for (−)-**2** (Fig. 5) led to the assignment of its absolute configuration as 6*R*,7*S*,8*S*,9*R*,10*R*. In the case of compound **2**, even the small positive Cotton effect at around 260 nm was correctly reproduced by quantum chemical calculations.

Compound **3**, named macrocephalide C, was obtained as an oil, with $[\alpha]_D^{24}$ −100 (*c* 0.2, $CHCl_3$). Its molecular formula, $C_{20}H_{24}O_8$, was deduced from the protonated molecular ion at *m/z* 393.1540 $[M+H]^+$ (calcd for $C_{20}H_{25}O_8$ *m/z* 393.1544) in the HR-ESI-MS, and from its ^{13}C NMR data.

Compound **3** exhibited the same molecular formula as that of **2**, which suggested that both compounds have similar structural features. Comparison of NMR spectroscopic data of **3** with those of compounds **1** and **2** (Table 1) revealed that **3** also possesses an α-methylene-γ-lactone moiety due to the signals at δ_C 168.4 (C=O), δ_C 134.3 (C-11), and at δ_H 6.39 (d, J = 3.0 Hz, H-13a) and 5.75 (d, J = 3.0 Hz, H-13b), both correlated with C-13 (δ_C 122.9) in the HMBC spectra. This comparison permitted also to evidence the presence of a 2-hydroxymethyl-2-butenoyl group, as in compound **2**, from the signals at δ_H 6.47 (H-3′), δ_H 2.00 (H-4′) and δ_H 4.13 and 4.17 (H-5’), together with those at δ_C 167.5 (C=O, C-1′), 130.5 (C-2′) and 143.6 (C-3′). The HMBC correlations (Figures S-27, S-28, and S-29, Supporting Information) of the signals at δ_H 2.00 (H-4′), δ_H 4.13 and 4.17 (H-5’) with C-2’ (δ_C 130.5), and δ_H 6.47 (H-3′) with C-5’ (δ_C 64.1) confirmed the assignments of chemical shifts for this group. Despite some structural similarity of **3** when compared to **1** and **2**, significant differences were observed in its NMR data concerning the germacranolide skeleton. The main differences were the absence of the resonances for the carbonyl group at C-1 and for hydrogens and carbons of the conjugated double bonds between C-2/C-3 and

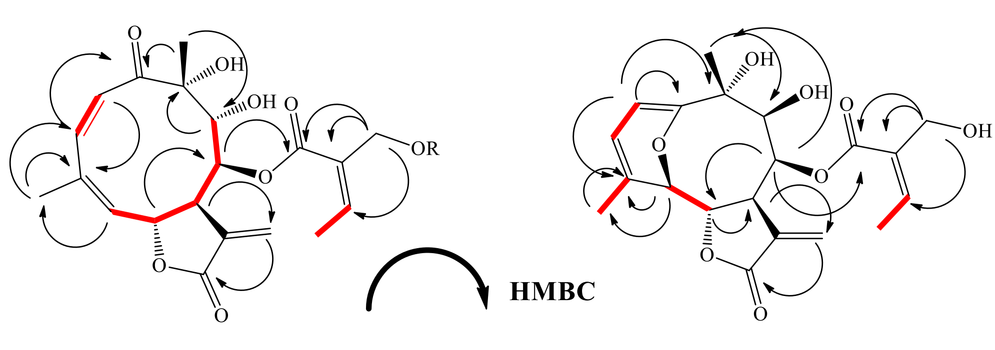

1 R = Ac
2 R = H
3

Fig. 2. Selected HMBC and COSY correlations of compounds **1**–**3**.

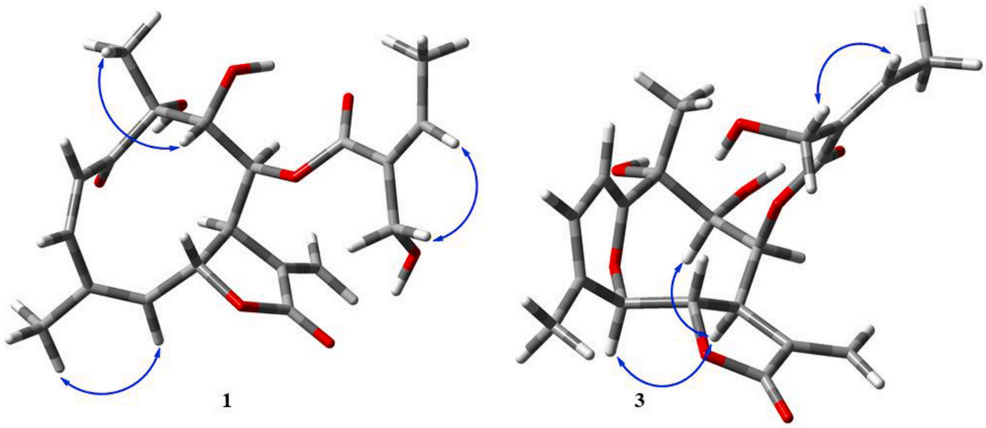

Fig. 3. Selected NOESY correlations of compounds **1** and **3**.

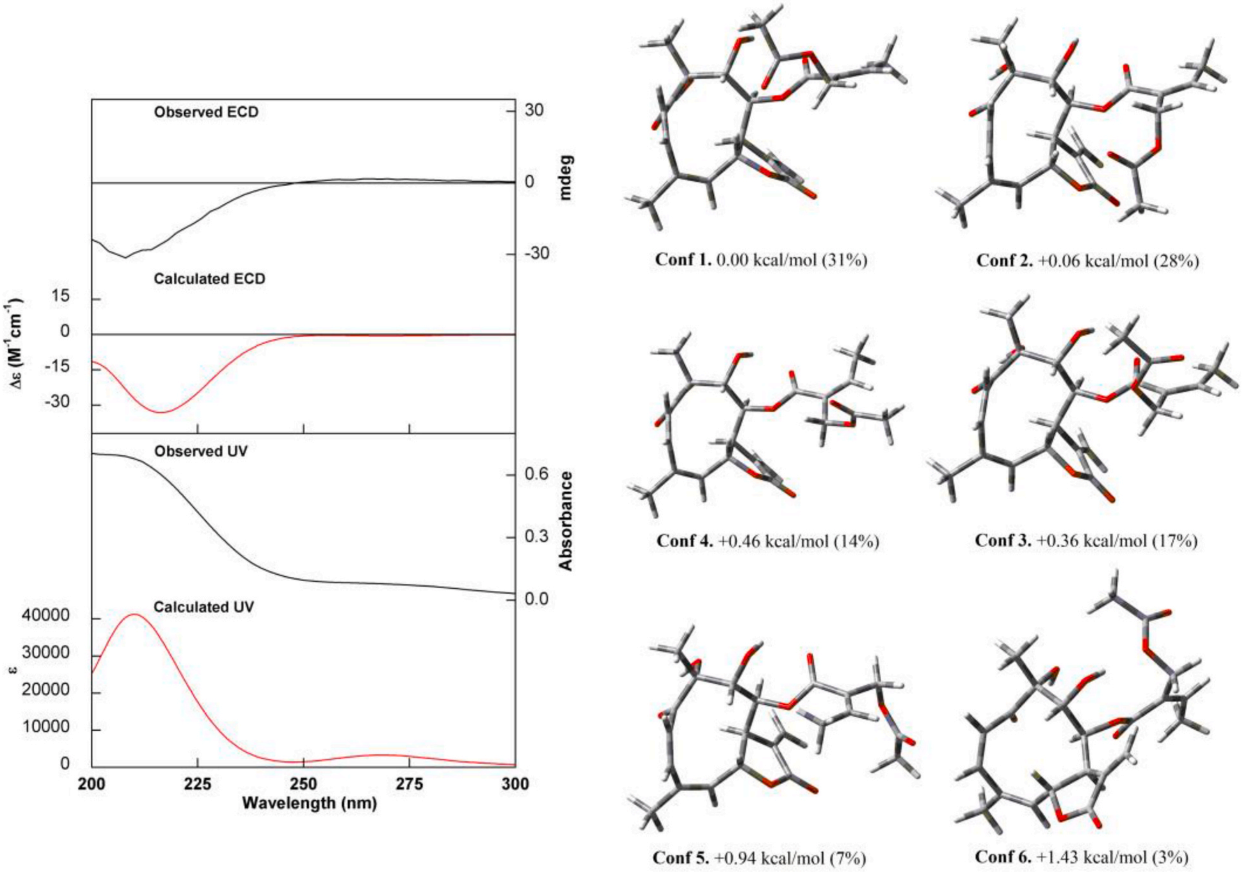

Fig. 4. (Left) Comparison of experimental UV and ECD spectra of (−)-**1** (black) with calculated (CAM-B3LYP/PCM(MeOH)/TZVP, red) spectra for (6*R*,7*S*,8*S*,9*R*,10*R*)-**1**. (Right) Optimized structures, relative energies and Boltzmann populations of the lowest-energy conformers identified for (6*R*,7*S*,8*S*,9*R*,10*R*)-**1** at the B3LYP/6-31G(d) level. (For interpretation of the references to colour in this figure legend, the reader is referred to the Web version of this article.)

C-4/C-5, which suggests a modification in the germacranolide skeleton at positions C-1 to C-5 for compound **3**. This proposal was corroborated by the presence of unexpected signals of a quaternary carbon at δ_C 150.7 and of two carbons of the double bond at δ_C 105.4 and 117.5, which are correlated, respectively, to the hydrogens at 5.72 (d, 5.5 Hz, H-2) and 5.87 (m, H-3) in the HSQC spectra. Also, the NMR spectra of **3** showed signals for four oxymethine groups [δ_H 4.15/δ_C 76.6; δ_H 4.41/δ_C 80.6; δ_H 4.93/δ_C 79.5 and δ_H 5.87/δ_C 75.0], while three oxymethine carbons were present in the structures of the compounds **1** and **2**. These data suggested the presence of an oxygen bridge between C-1 and C-5, with a formation of a six membered ring, which was confirmed by the HMBC correlations between the signals at δ_H 5.72 (H-2), 5.87 (H-3) and δ_H 4.15 (H-5) with δ_C 150.7 (C-1); δ_H 5.72 (H-2) with δ_C 133.6 (C-4); δ_H 4.15 (H-5) with δ_C 117.5 (C-3) and 133.6 (C-4). The oxymethyne carbon at δ_C 76.6 was assigned to C-5 from the correlation to δ_H 4.15 (H-5) in HSQC spectra. Further analysis of COSY and HMBC data permitted to complete the assignment of the hydrogens and carbons for germacranolide skeleton of **3**. The oxymethyne at δ_H 4.93/δ_C 79.5 was assigned to H-6/C-6 from the COSY and HMBC correlations of δ_H 4.93 with H-5 (δ_H 4.15) and with C-5 (δ_C 76.6), respectively. The assignments of H-7/C-7 were

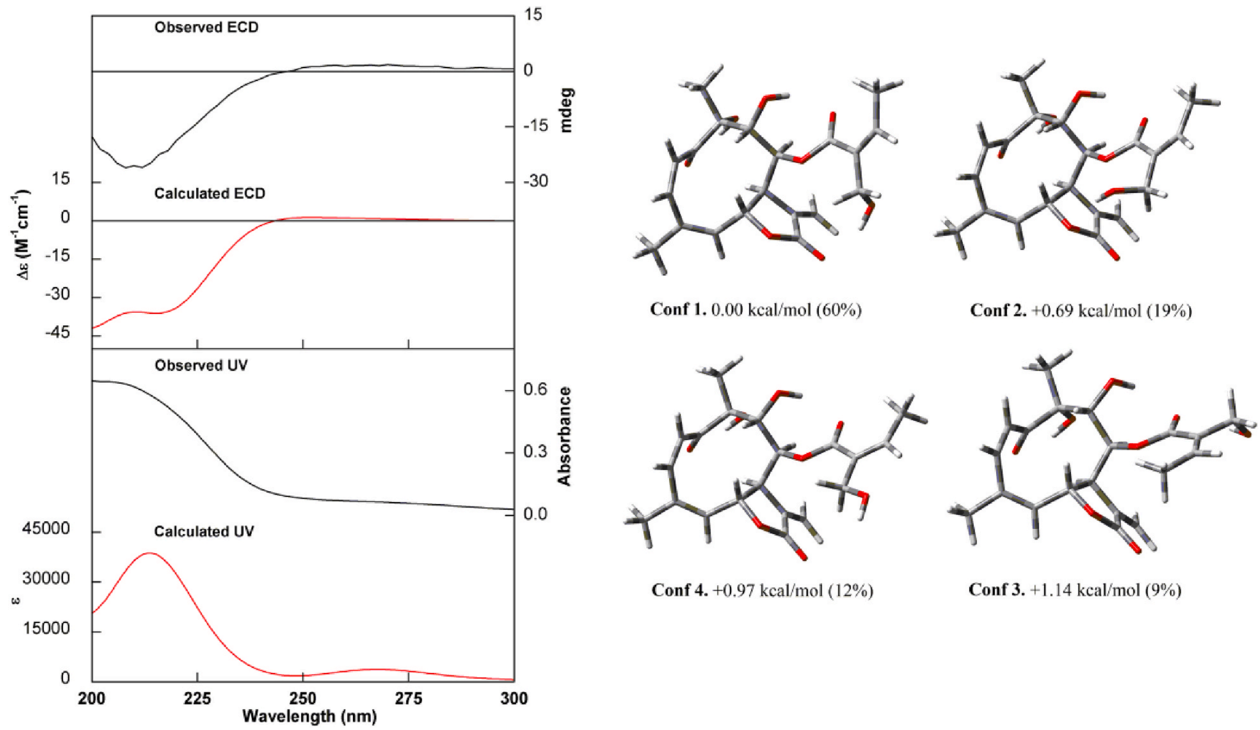

Fig. 5. (Left) Comparison of experimental UV and ECD spectra of (−)-**2** (black) with calculated (CAM-B3LYP/PCM(MeOH)/TZVP, red) spectra for (6*R*,7*S*,8*S*,9*R*,10*R*)-**2**. (Right) Optimized structures, relative energies and Boltzmann populations of the lowest-energy conformers identified for (6*R*,7*S*,8*S*,9*R*,10*R*)-**2** at the B3LYP/6-31G(d) level. (For interpretation of the references to colour in this figure legend, the reader is referred to the Web version of this article.)

supported from the COSY correlations (Figures S-30, S-31, and S-32, Supporting Information) of the hydrogen at δ_H 3.38 (H-7) with δ_H 4.93 (H-6) and at long-range with δ_H 6.39 and 5.75 (H-13), together with HSQC correlation between H-7 and the carbon at δ_H 49.2 (C-7). The oxymethynes at δ_H 5.87/δ_C 75.0 and δ_H 4.41/δ_C 80.6 were assigned to H-8/C-8 and H-9/C-9, respectively, based on HMBC correlation of the signal at δ_H 5.87 (H-8) with C-6 (79.5), and at δ_H 1.30 (CH_3-14) with the signal at δ_C 80.6. The HMBC correlation from H-2 and H-8 to the quaternary carbon at δ_C 74.1 evidenced this carbon as C-10. The HMBC correlation of the methyl hydrogens at δ_H 1.30 (14-CH_3) with the carbon C-1 confirmed the assignment and positioning of this group at C-10 (δ_C 74.1). The H-8 and H-14 hydrogens were correlated with the oxygenated carbons at δ_C 80.6 (CH) and δ_C 74.1 (C_0) in the HMBC spectra, confirming the assignment of these signals to C-9 and C-10, respectively. HMBC correlations of the methyl group at δ_H 2.02 (15-CH_3) with C-5 confirmed the attachment of this group at C-4. Finally, the positioning of the 2-hydroxymethyl-2-butenoyl group at C-8 was established by the correlation of H-8 (δ_H 5.87) with the carbonyl carbon C-1' (δ_C 167.5).

The NOESY spectra of compound **3** showed correlation of and H-7 (δ_H 3.38, m) with H-5 (δ_H 4.15) and H-9 (δ_H 4.41) (Fig. 3). The correlations between H-3' (δ_H 6.47) and H-5' (δ_H 4.13; 4.17) indicated a *Z* configuration for the C-2'/C-3' double bond, as observed for compounds **1** and **2**. In order to determine the absolute configuration of **3**, comparisons of experimental and simulated ECD spectra were performed. The excellent agreement between the ECD spectra obtained for (−)-**3** in methanol with that simulated for the 5*R*,6*S*,7*S*,8*S*,9*S*,10*R* configuration at the CAM-B3LYP/PCM(MeOH)/TZVP level (Fig. 6) allowed the assignment of (−)-**3** as 5*R*,6*S*,7*S*,8*S*,9*S*,10*R*.

Macrocephalide C (**3**) contains an undescribed type of germacranolide skeleton, and a proposed pathway for its formation is shown in Fig. 7. The suggested pathway was based in the UHPLC-HRMS/MS analysis of the dichloromethane fraction, from which **3** was isolated. From this analysis, a peak was observed for a protonated ion at *m/z* 411.1646 $[M+H]^+$ with the same fragmentation pattern as that of compounds **1** and **2**, which is consistent with the structure of the proposed precursor for **3**. The opening of epoxide ring of the precursor followed by intramolecular cyclization, and subsequent water elimination, provided compound **3**.

2.2. Antiproliferative activity

Following the protocol developed by the National Cancer Institute for antiproliferative screening of new anticancer drugs (Fouche et al., 2008; National Cancer Institute, 2015), we evaluated the antiproliferative potential of the isolated germacranolides **1**–**3**, against a panel of human tumor and non-tumor cell lines. According to this protocol, the concentration required to inhibit 50% of cell growth (GI_{50}) was calculate for each cell line to express the cytostatic effect of each sample.

Compounds activities were classified considering the GI_{50} value expressed as logarithm following the NCI's criteria for weak ($1.1 < \log GI_{50} < 1.5$), moderate ($0 < \log GI_{50} < 1.1$) and potent ($\log GI_{50} < 0$) activities (Fouche et al., 2008). Besides, considering the cytostatic effect on immortalized keratinocytes HaCaT, we calculated the selectivity index (SI) that relates the concentration required to inhibit 50% of HaCaT proliferation and that required for one tumor cell line, in the same experiment. This parameter allows presuming whether sample would affect normal proliferative tissues (Muller and Milton, 2012).

The macrocephalides A (**1**) and B (**2**) exhibited moderate to potent antiproliferative profile, inhibiting 50% of cell growth (GI_{50}) at concentrations ranging from 0.576 to 6.37 μM (Table 2). Macrocephalide A (**1**) inhibited more selectively the growth of melanoma (UACC-62, GI_{50} = 0.576 μM, SI = 1.8) and kidney (786–0, GI_{50} = 0.576 μM, SI = 1.8) tumor cells while compound **2** showed higher activity for adenocarcinoma ovarian cells (OVCAR-03, GI_{50} = 0.637 μM, SI = 6.3). Compound **3** was the least active weakly inhibiting renal (786–0, GI_{50} = 10.3 μM, SI = 6.2), leukemic (K562, GI_{50} = 14.6 μM, SI = 4.4), ovarian (OVCAR-03, GI_{50} = 15.7 μM, SI = 4.1) and melanoma (UACC-62, GI_{50} = 22.3 μM, SI = 2.9) cell lines (Table 2). Considering their molecular structure, the macrocyclic nuclei in macrocephalides A and B seemed to be important

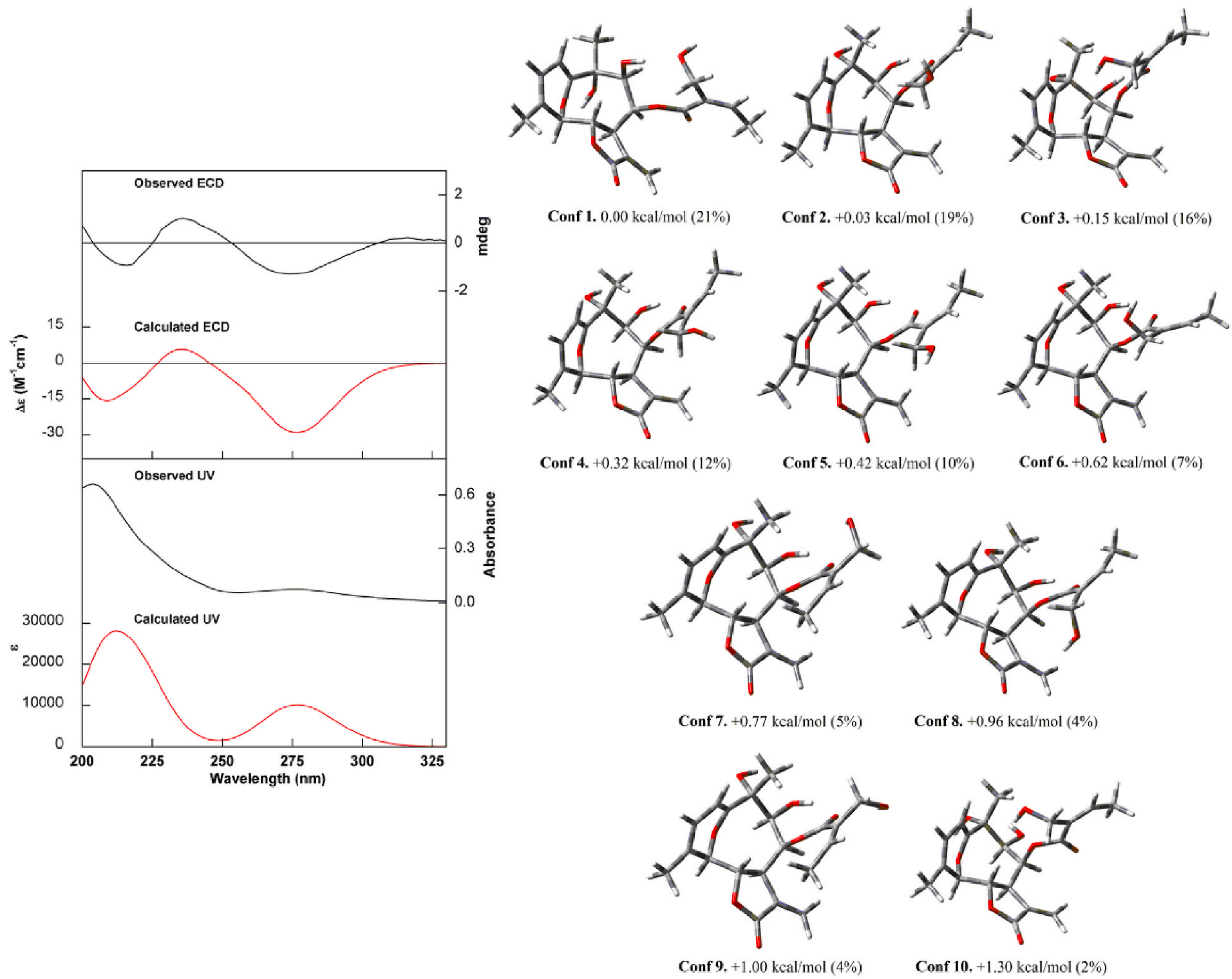

Fig. 6. (Left) Comparison of experimental UV and ECD spectra of (−)-**3** (black) with calculated (CAM-B3LYP/PCM(MeOH)/TZVP, red) spectra for (5*R*,6*S*,7*S*,8*S*,9*S*,10*R*)-**3**. (Right) Optimized structures, relative energies and Boltzmann populations of the lowest-energy conformers identified for (5*R*,6*S*,7*S*,8*S*,9*S*,10*R*)-**3** at the B3LYP/6-31G(d) level. (For interpretation of the references to colour in this figure legend, the reader is referred to the Web version of this article.)

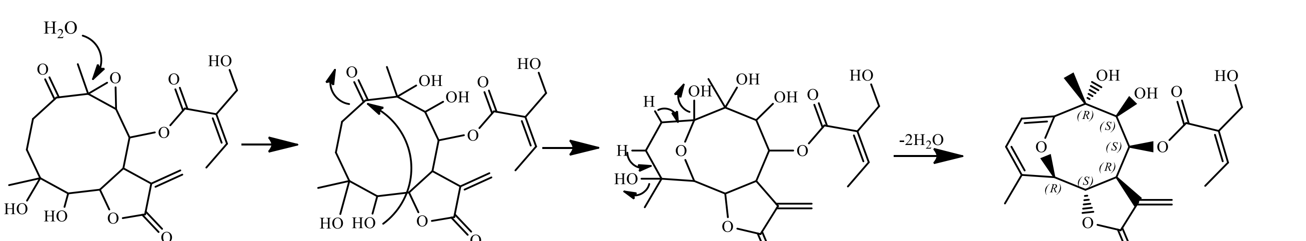

m/z 411.1646 [M+H]$^+$ **3**

Fig. 7. A proposed pathway for compound **3**.

for the antiproliferative activity while the substituents modulated this activity.

3. Conclusion

In summary, phytochemical investigation on *Campuloclinium macrocephalum* resulted in the isolation of three undescribed germacranolide sesquiterpene lactones (**1**–**3**), along with known steroids and triterpenes (**4**–**10**), and the flavonoids taxifolin (**11**) and quercetin-3-*O*-*α*-L-rhamnopyranoside-7-*O*-*β*-D-glucopyranoside (**12**). Antiproliferative assays showed that compound **1** inhibited more selectively the growth of melanoma (UACC-62, GI_{50} = 0.576 μM, SI = 1.8) and kidney (786–0, GI_{50} = 0.576 μM, SI = 1.8) tumor cells, and compound **2** showed higher activity for adenocarcinoma ovarian cells (OVCAR-03, GI_{50} = 0.637 μM, SI = 6.3). Our findings corroborate the properties of SLs as antitumor compounds, and may also to contributes with their ecological roles, since that the effect of *C. macrocephalum* against phytopathogenic fungi are already described.

Table 2
Antiproliferative activity of germacranolides **1**, **2** and **3** expressed as concentration required for 50% of cell growth inhibition (GI_{50}, μM) besides the selectivity index.

Human Cell line	Doxorubicin[a]			1			2			3		
	GI_{50}[b]	log GI_{50}[c]	SI[d]	GI_{50}[b]	log GI_{50}[c]	SI[d]	GI_{50}[b]	log GI_{50}[c]	SI[d]	GI_{50}[b]	log GI_{50}[c]	SI[d]
U251	0.09 ± 0.03	−1.0	5.2	5.76*	0.7	0.2	6.37*	0.8	0.6	61.5 ± 10.3	1.8	1.0
UACC-62	<0.046	<-1.4	>12.4	0.576*	−0.2	1.8	n.t.	n.t.	n.c.	22.3 ± 10.9	1.3	2.9
MCF-7	<0.046	<-1.3	>10.0	1.5 ± 0.7	0.2	0.7	3.5 ± 0.9	0.5	1.1	55.8 ± 0.5	1.7	1.1
NCI-ADR/RES	0.46 ± 0.01	−0.3	1.0	1.1 ± 0.5	0.07	0.9	1.6 ± 0.3	0.2	2.6	91.0 ± 36.6	2.0	0.7
786-O	<0.046	<-1.3	>10.0	0.576*	−0.2	1.8	1.2 ± 0.5	0.1	3.4	10.3 ± 0.4	1.0	6.2
NCI–H460	<0.046	<-1.3	>10.0	5.76*	0.8	0.2	6.37*	0.8	0.6	63.7*	1.8	1.0
OVCAR-03	0.46*	−0.3	1.0	5.76*	0.8	0.2	0.637*	−0.2	6.3	15.7 ± 3.4	1.2	4.1
HT29	0.77 ± 0.16	−0.1	0.6	2.3 ± 0.6	0.4	0.5	4.7 ± 0.6	0.7	0.9	63.7*	1.8	1.0
K562	0.46*	−0.3	1.0	5.76*	0.8	0.2	6.37*	0.8	0.6	14.6 ± 3.0	1.2	4.4
HaCaT	0.46*	−0.3 P	n.a.	1.05 ± 0.09	0.02	n.a.	4.0 ± 0.5	0.6	n.a.	63.7*	1.8	n.a.

*approximated value; n.t.: not tested; n.c.: not calculated; n.a.: not applied. Human tumor cell lines: U251 (glioblastoma); UACC-62 (melanoma); MCF-7 (breast, adenocarcinoma); NCI-ADR/RES (ovary, multi-drug resistant adenocarcinoma); 786–0 (kidney, adenocarcinoma); NCIH460 (lung, large cell carcinoma), OVCAR-03 (ovary, adenocarcinoma), HT-29 (colon, adenocarcinoma), K562 (chronic myeloid leukemia). Human non-tumor cell lines: HaCaT (immortalized keratinocyte).

[a] Doxorubicin: chemotherapeutic drug.

[b] GI_{50}: Growth Inhibition 50, expressed in μM followed by standard error, calculated by sigmoidal regression using Origin 8.0 software.

[c] log GI_{50}: results expressed as logarithm and classified according to b NCI's criteria (weak activity: $1.1 < \log GI_{50} < 1.5$; moderate activity: $0 < \log GI_{50} < 1.1$; potent activity: $\log GI_{50} < 0$).

[d] SI: selectivity index calculated as $GI_{50\ HaCaT}/GI_{50\ Tumor\ cell\ line}$.

4. Experimental section

4.1. General experimental procedures

Optical rotations were measured at 24 °C on a PerkinElmer Model 343 polarimeter. 1D and 2D NMR spectra were recorded in CD_3OD, DMSO-d_6 and $CDCl_3$ in a Bruker 500 MHz NMR instrument (Avance 500). High-resolution mass spectra were obtained in a QTOF, Bruker Daltonics, model Impact II spectrometer in electrospray ionization. C18 columns (75 × 2.0 mm i.d.; 1.6 μm Shim-pack XR-ODS III) were used for UHPLC separation using a Shimadzu, model Nexera X2. Silica gel 60 (0.063–0.200 mm) and silica gel 60 (0.04–0.063 mm) were used for purification of the compounds. TLC was performed on normal phase pre-coated silica gel 60 G or 60 GF_{254} (Merck) plates. The UV and ECD spectra of **1**–**3** were recorded with a Jasco J-815 spectrometer (Jasco, Tokyo, Japan) in the 195–400 nm region using the following parameters: bandwidth 1 nm; 25 response 1 s; scanning speed 100 nm min^{-1}; 3 accumulations; room temperature; sample in methanol solution; 0.1 cm cell path length; concentration 0.2 mg mL^{-1}.

4.2. Plant material

The plant material (aerial parts) of *Campuloclinium macrocephalum* (Less.) DC., Asteraceae, was collected in *Campos Gerais* National Park (25°08′46″ S, 049°057′025″ W), Paraná State, Brazil on March 2012 and identified by Dr. Marta Regina Barrotto do Carmo (Departamento de Biologia Geral, Universidade Estadual de Ponta Grossa). A voucher specimen (HUPG, 18905) has been deposited at the at the HUPG herbarium.

4.3. Extraction and isolation

The air-dried powder of aerial parts of *C. macrocephalum* (698.9 g) was extracted with methanol (2 × 2.5 L), at room temperature, and the solvent evaporated under vacuum. The methanol extract (17 g) was dissolved in methanol: water (50:50) and partitioned into *n*-hexane, dichloromethane and ethyl acetate. Evaporation of the solvents resulted in the *n*-hexane (CM-HF, 4.95 g), dichloromethane (CM-DF, 2.33 g), ethyl acetate (CM-EAF, 2.15 g) and aqueous-methanol (CM-AMF, 7.14 g) fractions. Part of the dichloromethane fraction (931 mg) was subjected to silica gel column chromatography using a gradient solvent system of *n*-hexane-acetone (98:2 to 0:100) to afford the subfractions CM-DF.1 to CM-DF.11. Purification of subfraction CM-DF.8 (277 mg) on silica gel *flash* CC, using a mixture of *n*-hexane−acetone (95:5 to 10:90) and acetone as eluent, afforded compounds **1** (5 mg) and **2** (5 mg). Another part of the dichloromethane fraction (450 mg) was subjected to silica gel CC using a gradient solvent system of *n*-hexane-acetone (98:2 to 0:100), to afford subfractions CM-DF.1 to CM-DF.11. Purification of CM-DF.5 (32 mg) on Sephadex LH-20, using methanol/water (50:50) gave compound **3** (8 mg). The hexane fraction was subjected to silica gel CC eluted with a mixture of *n*-hexane/ethyl acetate (95:5 to 10:90), to afford the subfractions CM-HF.1 to CM-HF.10. The subfractions CM-HF.3 and CM-HF.4 provided, respectively, a mixture of **4**, **5** and **6** (48.1 mg) and **7**, **8**, **9** and **10** (50.1 mg). The ethyl acetate fraction was subjected to purification in Sephadex LH-20 eluted with a mixture of methanol/water (10:90 to 90:10), to afford the subfractions CM-AEF.1 to CM-AEF.7. The subfraction CM-FAE.6 afforded compound **11** (5 mg). Part of methanol-aqueous fraction (1.2 g) was subjected to filtration in Sephadex LH-20 using methanol/water (10:90 to 90:10) to afford the subfractions CM-AMF.1 to CM-AMF.7. Purification of subfraction CM-AMF.2 (60 mg) by Sephadex LH-20 using a mixture of methanol/water (50:50) afforded compound **12** (3 mg).

Macrocephalide A (**1**): $[\alpha]_D^{24} = -117$ (*c* 0.7, chloroform) ^1H and ^{13}C NMR see Table 1; HR-ESI-MS *m/z* 435.1651 $[M + H]^+$ (calcd for $C_{22}H_{27}O_9$, 435.1650).

Macrocephalide B (**2**): $[\alpha]_D^{24} = -150$ (*c* 0.4, chloroform) ^1H and ^{13}C NMR see Table 1; HR-ESI-MS *m/z* 393.1543 $[M + H]^+$ (calcd for $C_{20}H_{25}O_8$, 393.1544).

Macrocephalide C (**3**): $[\alpha]_D^{24} = -100$ (*c* 0.2, chloroform) ^1H and ^{13}C NMR see Table 1; HR-ESI-MS *m/z* 393.1540 $[M + H]^+$ (calcd for $C_{20}H_{25}O_8$, 393.1544).

4.4. Calculations of ECD spectra

All density functional theory (DFT) and time-dependent-DFT (TDDFT) calculations were carried out at 298 K in the gas phase with Gaussian 09 software (Frisch et al., 2009). Calculations were performed for the arbitrarily chosen (6*R*,7*S*,8*S*,9*R*,10*R*)-**1**, (6*R*,7*S*,8*S*,9*R*,10*R*)-**2** and (5*R*,6*S*,7*S*,8*S*,9*S*,10*R*)-**3**. Conformational searches were carried out at the molecular mechanics level of theory with the Monte Carlo algorithm employing the MM + force field incorporated in HyperChem 8.0.10 software package. Initially, 100 conformers of (6*R*,7*S*,8*S*,9*R*,10*R*)-**1** with relative energy (rel E.) within 10 kcal mol^{-1} of the lowest-energy conformer were selected and further geometry optimized at the B3LYP/6-31G(d) level. The six conformers with rel E. <2.5 kcal mol^{-1}, which corresponded to more than 93% of the total Boltzmann distribution, were selected for UV and ECD spectral calculations. As for **2**, the same six lowest-energy conformers identified for **1** were selected.

Then, their acetate group at C-5' was replaced with a hydroxyl group, followed by further geometry optimization at the B3LYP/6-31G(d) level resulting in four conformers with rel E. within 2.0 kcal mol^{-1}. Regarding **3**, 56 conformers of (5*R*,6*S*,7*S*,8*S*,9*S*,10*R*)-**3** with rel E. within 10 kcal mol^{-1} of the lowest-energy conformer were selected and further geometry optimized at the B3LYP/6-31G(d) level. The ten conformers with rel E. <1.3 kcal mol^{-1}, which corresponded to more than 82% of the total Boltzmann distribution, were selected for UV and ECD spectral calculations. Vibrational analysis at the B3LYP/6-31G(d) level resulted in no imaginary frequencies for all conformers, confirming them as real minima. TDDFT was employed to calculate the excitation energy (in nm) and rotatory strength R in the dipole velocity (R_{vel} in cgs units: 10^{-40} esu^2 cm^2) form, at the CAM-B3LYP/PCM(MeOH)/TZVP level. The calculated rotatory strengths from the first 30 singlet → singlet electronic transitions were simulated into an ECD curve using Gaussian bands with a bandwidth of σ 0.25 eV. The predicted wavelength transitions were used without any scaling. The Boltzmann factor for each conformer was calculated based on Gibbs free energies.

4.5. Antiproliferative assay

The antiproliferative activities of compounds **1**, **2** and **3** were evaluated *in vitro* against nine different human cancer cell lines [U251 (glioma), UACC-62 (melanoma), MCF-7 (breast), NCI/ADR-RES (ovarian expressing multiple-drug-resistance phenotype), 786–0 (renal), NCI–H460 (non-small cell lung cancer), OVCAR-3 (ovarian), HT-29 (colon) and K562 (leukemia)]. The tumor cell lines were provided by Frederick Cancer Research & Development Center, National Cancer Institute, Frederick, MA, USA. The antiproliferative activities were also evaluated using a non-tumor cell line HaCat (human keratinocyte), provided by Dr. Ricardo Della Coletta (University of Campinas- UNICAMP, Brazil). Stock and experimental cultures were grown in complete medium containing 5 mL RPMI 1640 (GIBCO BRL) supplemented with 5% fetal bovine serum (GIBCO BRL) and 1% Penicillin:Streptomycin mixture (1000 $U.mL^{-1}$:1000 $\mu g.mL^{-1}$). The sample were previously diluted in DMSO (100 $mg\cdot mL^{-1}$) followed by serial dilution in complete medium, affording the final concentrations of 0.576, 5.76, 57.6 and 576 μM for compound **1**, and 0.637, 6.37, 63.7 and 637 μM for compounds **2** and **3**. Cells in 96-well plates (100 μL cells $well^{-1}$, inoculation density: 3.5 to 6 x 10^4 $cell\cdot mL^{-1}$, Table S4, in Supplementary material) were exposed to sample for 48 h, in triplicate, at 37 °C, 5% of CO_2 in air. The final DMSO concentration (<0.25%) did not affect cell viability. Doxorubicin (0.046–0.46 μM) was used as positive control. Before (T_0 plate) and after the sample addition (T_1 plates), cells were fixed with 50% trichloroacetic acid, and cell proliferation was determined by spectrophotometric quantification (540 nm) of cellular protein using the sulforhodamine B assay. Cell proliferation was calculated considering (T_1 - T_0) as representing 100% of cell growth when absorbance of treated cells (T_S) was higher than T_0 absorbance; more, when absorbance of treated cells (T_S) was lower than T_0 absorbance, 100% of cell growth was represented by T_0. For each sample, one concentration–response curve correlating sample concentration with cell growth was plotted using the software ORIGIN 8.0® (OriginLab Corporation) (Monks et al., 1991). The Selectivity Index (SI) was estimated as SI = GI_{50}(HaCat)/GI_{50}(cancer cell line) (Muller and Milton, 2012).

Declaration of competing interest

The authors declare that they have no known competing financial interests or personal relationships that could have appeared to influence the work reported in this paper.

Acknowledgments

The authors thank Coordenação de Aperfeiçoamento de Pessoal de Nível Superior (CAPES, Brazil, Finance code 001) and Conselho Nacional de Desenvolvimento Científico e Tecnológico (CNPq, Brazil) for financial support. JMBJ thanks Fundação de Amparo à Pesquisa do Estado de São Paulo (FAPESP) for funding (grant# 2014/25222–9). This work was supported by the Complexo de Central de Apoio à Pesquisa (COMCAP) from the Universidade Estadual de Maringá (UEM). This research was also supported by resources supplied by the Centre for Scientific Computing (NCC/GridUNESP) of São Paulo State University (UNESP).

Appendix A. Supplementary data

Supplementary data related to this article can be found at https://doi.org/10.1016/j.phytochem.2020.112469.

References

Agrawal, P.K., 1989. Carbon-13 NMR of Flavonoids, Studies in Organic Chemistry, vol. 39. Elsevier Science, p. 39.

Breedlove, D.E., 1986. Listados Florísticos de México, vol. 4, pp. 1–246.

Cabrera, A.L., 1974. Flora Ilustrada de Entre Rios, vol. 6, pp. 106–540.

Cabrera, A.L., 1978. Flora de la provincia de Jujuy (Compositae). Colección Científica. Inst Nal Tec Agr 13 (10), 1–726.

Fouche, G., Cragg, G.M., Pillay, P., Kolesnikova, N., Maharaj, V.J., Senabe, J., 2008. *In vitro* anticancer screening of South African plants. J. Ethnopharmacol. 28 (119), 455–461. https://doi.org/10.1016/j.jep.2008.07.005.

Freire, S.E., 2008. Tribu Eupatorieae (Asteraceae). In: Zuloaga, F.O., Morrone, O., Belgrano, M. (Eds.), Catálogo de las Plantas Vasculares del Cono Sur de América del Sur: Argentina, Sur de Brasil (Paraná, Santa Catarina y Rio Grande do Sul), Chile, Paraguay y Uruguay. Monographs in Systematic Botany from the Missouri Botanical Garden, vol. 114, pp. 1277–1302.

Frisch, M.J., Trucks, G.W., Schlegel, H.B., et al., 2009. Gaussian 09, Revision A.02. Gaussian, Inc., Wallingford CT.

Gonzalez, T.D., 1992. Catálogo de plantas medicinais usadas no Paraguay. Comuneros, Asunción.

Gonzalez, A.G., Bermejo, J., Breton, J.L., Massanet, G.M., 1972. Chemistry of the compositae. XI. *Eupatorium macrocephalum* less. *An. Quim. Int. Ed.* 68 (3), 319–323.

Gonzalez, A.G., Bermejo, J., Massanet, G.M., 1973. Chemistry of the compositae. XIV. Flavonoids of *Eupatorium macrocephalum* Less. *An. Quim.* 69 (2), 229–234.

Goodall, J., Witkowski, E.T.F., Ammann, S., Reinhardt, C., 2010. Does allelopathy explain the invasiveness of *Campuloclinium macrocephalum* (pompom weed) in the South African grassland biome? Biol. Invasions 12, 3497–3512. https://doi.org/10.1007/s10530-010-9747-2.

Hensel, A., Maas, M., Sendker, J., Lechtenberg, M., Petereit, F., Deters, A., Schmidt, T., Stark, T., 2011. *Eupatorium perfoliatum* L.: phytochemistry, traditional use and current Applications. J. Ethnopharmacol. 138, 641–651. https://doi.org/10.1016/j.jep.2011.10.002.

Huo, J., Yang, S.P., Ding, J., Yue, J.M., 2004. Cytotoxic sesquiterpene lactones from *Eupatorium lindleyanum*. J. Nat. Prod. 67, 1470–1475. https://doi.org/10.1021/np040023h.

Liu, P.Y., Liu, D., Wei-Huan Li, W., Zhao, T., Sauriol, F., Gu, Y., Shi, W., Zhang, M., 2015. Chemical constituents of plants from the genus *eupatorium* (1904–2014). *Chem. Biodivers.* 12, 1481–1514. https://doi.org/10.1002/cbdv.201400227.

Mahato, S.B., Kundu, A.P., 1994. 13C NMR spectra of pentacyclic triterpenoids-a compilation and some salient features. Phytochemistry 37, 1517–1575. https://doi.org/10.1016/S0031-9422(00)89569-2.

Mdee, L.K., Masoko, P., Eloff, J.N., 2009. The activity of extracts of seven common invasive plant species on fungal phytopathogens. *S. Afr. J. Bot.* 75, 375–379. https://doi.org/10.1016/j.sajb.2009.02.003.

Monks, A., Scudiero, D., SKehan, P., Shoemaker, R., Paull, K., Vistica, D., Hose, C., Langley, J., Cronise, P., Vaigro-Wolff, A., Gray-Goodrich, M., Campbell, H., Mayo, J., Boyd, M., 1991. Feasibility of a high-flux anticancer drug screen using a diverse panel of cultured human tumor cell lines. J. Natl. Cancer Inst. 83, 757–766. https://doi.org/10.1093/jnci/83.11.757.

Muller, P.Y., Milton, M.N., 2012. The determination and interpretation of the therapeutic index in drug development. Nat. Rev. Drug Discov. 11, 751-761. https://doi.org/10.1038/nrd3801.

National Cancer Institute - NCI, 2015. Developmental Therapeutics Program. Standard Operating Procedures for Sample Preparation for NCI60 Screen. Accessed in 06/14/19, Available at: https://dtp.cancer.gov/discovery_development/nci-60/handling.htm.

Saito, Y., Mukai, T., Iwamoto, Y., Baba, M., Takiguchi, K., Okamoto, Y., Gong, X., Kawahara, T., Kuroda, C., Tori, M., 2014. Germacranolides and their diversity of *Eupatorium heterophyllum* collected in P. R. China,. Chem. Pharm. Bull. 62, 1092–1099. https://doi.org/10.1248/cpb.c14-00426.

Shen, Y.C., Lo, K.L., Kuo, Y.H., Khalil, A.T., 2005. Cytotoxic sesquiterpene lactones from *Eupatorium kiirunense*, a coastal plant of Taiwan. J. Nat. Prod. 68, 745–750. https://doi.org/10.1021/np040214k.

Vega, M.R.G., Carvalho, M.G., Vieira, E.J.C., Braz-Filho, E.R., 2008. Chemical constituents from the Paraguayan medicinal plant, *Eupatorium macrocephalum* Less. J. Nat. Med. 62, 122–123. https://doi.org/10.1007/s11418-007-0168-1.

Wang, F., Zhong, H., Fang, S., Zheng, Y., Li, C., Peng, G., Shen, X., 2018. Potential anti-inflammatory sesquiterpene lactones from *Eupatorium lindleyanum*. Planta Med. 84, 123–128. https://doi.org/10.1055/s-0043-117742.
Williams, L.O., 1976. Compositae of Central America–V. The genus *brickellia* (Eupatorieae) in Costa Rica. Fieldiana Bot. 24, 1–603.
Wu, H., Fronczek, F.R., Burandt Jr., C.L., Zjawiony, J.K., 2011. Antileishmanial germacranolides from *Calea zacatechichi*. Planta Med. 77, 749–753. https://doi.org/10.1055/s-0030-1250584.
Yamada, M., Matsura, N., Suzuki, H., Kurosaka, C., Hasegawa, N., Ubukata, M., Tanaka, T., Iinuma, M., 2004. Germacranolides from *Calea urticifolia*. Phytochemistry 65, 3107–3111. https://doi.org/10.1016/j.phytochem.2004.08.040.
Yu, X., Zhang, Q., Tian, L., Guo, Z., Liu, C., Chen, J., Ebrahim, W., Liu, Z., Proksch, P., Zou, K., 2018. Germacrane-type sesquiterpenoids with antiproliferative activities from *Eupatorium chinense*. J. Nat. Prod. 81, 85–91. https://doi.org/10.1021/acs.jnatprod.7b00693.
Zhang, M.L., Wu, M., Zhang, J.J., Irwin, D., Gu, Y.C., Shi, Q.W., 2008. Chemical constituents of plants from the genus *Eupatorium*. Chem. Biodivers. 5, 40–55. https://doi.org/10.1002/cbdv.200890014.